



Published in final edited form as:

*Biochemistry*. 2018 August 14; 57(32): 4867–4879. doi:10.1021/acs.biochem.8b00125.

## Adaptive Multifunctional Supramolecular Assemblies of Glycopeptides Rapidly Enable Morphogenesis

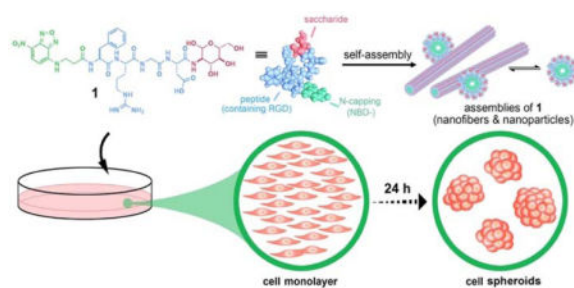
Jie Zhou<sup>‡</sup>, Xuewen Du<sup>‡</sup>, Xiaoyi Chen, and Bing Xu<sup>\*</sup>

Department of Chemistry, Brandeis University, 415 South Street, Waltham, MA 02453, USA

### Abstract

Despite the well-established biophysical principle of adhesion-guided in vitro morphogenesis, there are few single synthetic molecular species that can rapidly enable morphogenesis (e.g., a cell monolayer to cell spheroids) in cell culture because adhesion process inherently involves many signals. Here we show the use of adaptive multifunctional supramolecular assemblies of glycopeptides, consisting of cell adhesion sequence and saccharide, to induce cell spheroids rapidly from a monolayer of cells. Having a general architecture of N-terminal capping, glycosylation, and an integrin binding sequence, the glycopeptides self-assemble to form a dynamic continuum of nanostructures (i.e., from nanoparticles to nanofibers) to affect the interactions of integrins, E-selectin, and cadherins with their natural ligands and to act adaptively according to cellular environment. Such adaptive (i.e., context-dependent) interactions reduce cell-substratum adhesion and enhance intercellular interactions, which rapidly and transiently induce cell spheroids. This work illustrates a new approach that uses supramolecular assemblies of simple glycopeptides as molecular modulators of biophysical condition of cells for understanding and affecting cell functions in the development of supramolecular biomaterials.

### Graphical Abstract



Corresponding Author: bxu@brandeis.edu.

<sup>‡</sup>Author Contributions

These authors contributed equally.

Supporting Information

See supporting information for synthetic procedures, NMR and LC-MS characterization, and other supplementary results. This material is available free of charge via the Internet at <http://pubs.acs.org>

## Introduction

It is well established that intercellular interactions in three-dimension (3D) environment differ profoundly from the monolayer of cells (2D).<sup>1</sup> Increased reports suggests that 3D cell organization provides better in vitro models that represent more accurately the actual in vivo microenvironment<sup>2-7</sup> than 2D layers of cells. Such insights have led to the developed 3D in vitro models of human cells in hope to bridge the discontinuity in in vitro systems and in vivo animal models for the purpose of drug discovery, stem cell study, cancer cell biology, and tissue engineering and implantation.<sup>8-10</sup> There are two types of 3D cell models, one cultures cells on a 3D scaffold (e.g., microencapsulation,<sup>11-14</sup> stacked of layered papers,<sup>15</sup> or hydrogels<sup>16-19</sup>), the other is to form cell spheroids. The use of scaffolds is straightforward, but it is difficult to achieve high reproducibility. For example, the use of hydrogel scaffolds (e.g., Matrigels) has received the most exploration,<sup>20, 21</sup> but the animal origins of Matrigels may cause inconsistency<sup>22</sup> and is unable to recapitulate the biological features of human tumors.<sup>23, 24</sup> With the advancement of organoids,<sup>25</sup> there is renewed interests of generating cell spheroids as the 3D in vitro models of human cells.<sup>26, 27</sup> Although many efforts have focused on generating cell spheroids, the current procedures<sup>28-32</sup> are tedious, time-consuming, costly, or poorly controlled, thus it is necessary to develop a more general and effective approach for generating cell spheroids in vitro.

Obviously, the simplest and the most physiologically-relevant way to generate cell spheroids is spontaneous cell aggregation, as occurred during cell morphogenesis.<sup>33</sup> Despite that morphogenesis involves many biochemical signals, cell adhesion plays a crucial role in assembling individual cells into the three-dimension tissues or organs. Particularly, Griffith et al. have shown that cell-substratum and cell-cell adhesive forces are critical for 2D to 3D cell morphogenesis in vitro.<sup>34</sup> In fact, this well-established biophysical principle acts as the base for a variety of methods for generating cell spheroids, including hanging drops, spinner flasks, rotary culture, and low binding surface. Although these approaches have successfully generated cell spheroids based on the forces of cell adhesion,<sup>33</sup> they still have several drawbacks, such long incubation periods, limited sizes of the spheroids, and poor control of cell distribution. Considering that different biochemical interactions are able to result in same cell adhesion force as the biophysical determinant,<sup>34</sup> it should be feasible to use synthetic molecules to modulate cell adhesion forces for generating cell spheroids.

Based on the biophysical principle elucidated by Griffin et al.<sup>35</sup> and several results related to cell culture on peptide assemblies,<sup>36, 37</sup> small cell spheroids prompted by cell adhesion peptide<sup>38-41</sup> and sialylation,<sup>42, 43</sup> and in vitro morphogenesis induced by dynamic continuum of supramolecular phosphoglycopeptides,<sup>44</sup> we use the supramolecular assemblies of glycopeptides (e.g., **1**), consisting of an N-terminal capping group, a cell adhesion sequence (arginine-glycine-aspartic acid (RGD)),<sup>38, 39</sup> and a saccharide, to induce cell spheroids. Transmission electron microscopy (TEM) indicates the assemblies of the glycopeptides acting as a continuum of nanostructures (i.e., nanoparticles to nanofibers). Fluorescent imaging reveals that the glycopeptides conformably assemble on the cell surfaces, with higher density at the location of cell spheroids than at the cell monolayer. Actin staining indicates a morphological change in cell shape of the individual cells in

spheroids. Blocking the interactions between the glycopeptide assemblies and the cell adhesion proteins (E-selectin, cadherins, and integrins) by monoclonal antibodies (mAbs) or inhibitors efficiently abrogates the formation of the spheroids. Immunofluorescence staining of fibronectin suggests that the assemblies complement fibronectin in the cell spheroids. Dissociating the assemblies revert the cells from spheroids to a monolayer, confirming the transient action of the supramolecular assemblies. Molecular validation of the glycopeptides indicates that N-capping, glycosylation, and binding of integrins are crucial for the observed in vitro morphogenesis, which establishes a general designing principle of the glycopeptide assemblies for modulating cell adhesions. Cytotoxicity assay indicates that the spheroids exhibit higher resistance to anticancer drug than the monolayers, further validating that the cell spheroids resemble tumors in vivo. These results, collectively, indicate that being multifunctional and adaptively interacting with cell adhesion proteins, the glycopeptide assemblies simultaneously reduce cell adhesion to the sub-stratum and enhance intercellular interactions for generating the spheroids (Scheme 1 and Figure 1a). Illustrating a new approach to use supramolecular glycopeptide assemblies for modulating biophysical conditions of cells in context-dependent manner, this work also provides insights for developing multifunctional supramolecular assemblies to affect other cell functions or processes.

## Results and Discussion

### Molecular design and self-assembly

Recently, cyclic derivatives of cell adhesion peptides (RGD) have enabled the formation of 3D spheroids on agarose surface, but still requires long incubation time (e.g., 7 days).<sup>42</sup> Although the sizes of the spheroids induced by the RGD derivatives are small (e.g., 80  $\mu\text{m}$ ), the investigation on the case of prostate cancer cell spheroids by Szewczuk et al.<sup>43</sup> reveals that sialylation facilitates the formation of 3D spheroids in the presence of the cyclic RGD derivatives. In another study, Uesugi et al. reported that a derivative of RGDS is able to protect cells from anoikis for cell transplantation.<sup>41</sup> In addition, Zhang et al. have shown that the assemblies of peptides, consisting of RAD (exhibiting weaker affinity to integrins than RGD) repeats, are excellent scaffolds for cell adhesion.<sup>36</sup> These results confirm that cell adhesion sequences (e.g., RGD), saccharides, and supramolecular assemblies are able to modulate cell adhesion. Therefore, it is conceivable to combine them (i.e., cell adhesion sequences, saccharides, and supramolecular assemblies) to generate a single synthetic molecular species to enable morphogenesis in vitro. Thus, we decide to examine the supramolecular assemblies of glycosylated RGD for enabling morphogenesis in vitro. Besides the aforementioned results,<sup>34, 36, 40, 41, 43</sup> we choose the assemblies of glycosylated RGD because (i) cell organization and intercellular communication<sup>45–47</sup> in cell spheroids must be regulated by extracellular matrix (ECM) proteins,<sup>48–52</sup> which possess cell adhesion sequences and are usually glycosylated;<sup>53</sup> (ii) assemblies of small saccharides can mimic the binding and functions of glycans.<sup>54</sup>

Based on the above rationale, we design and synthesize a glycopeptide (**1**), which consists of (i) an N-terminal capping group (NBD), for visualizing the molecular distribution of the assemblies in cellular environment and for facilitating self-assembly of the glycopeptides,

(ii) RGD sequence, a well-established cell adhesion sequence<sup>55</sup> that exhibit paradoxical roles,<sup>56, 57</sup> for acting as a peptide backbone to promote the self-assembly to form nanoscale structures for cell adhesion, and (iii) a saccharide (D-glucosamine), not only for improving proteolytic stability of small peptides,<sup>58, 59</sup> but also, after self-assembly, for mimicking the roles of glycosylation of ECM proteins. To understand the functions of each segment in the glycopeptides (i.e., N-terminal capping, RGD domain, and saccharide), we also design molecules **2-15** as the analogs of **1** (Scheme 2 and Figure S1).

The hydrophilic motifs (glycoside and RGD domain) enable **1** to dissolve in water to give a clear orange solution, even at high concentrations (Figure S2a). TEM images (Figure 1b) show that **1** forms a mixture of nanoparticles and nanofibers at the concentration of 500  $\mu\text{M}$ . The dynamic nature of supramolecular assemblies would allow a continuous transition between these two species (i.e., a continuum). Lowering the concentration to 100  $\mu\text{M}$  results in fewer nanofibers but more amorphous aggregates (Figure S2b). C-terminal glycosylation, though slightly decreasing the self-assembly ability of the peptide, largely improves the proteolytic resistance of the peptides against proteinase K, a powerful protease (Figure S2c).

### Formation and imaging of the 3D cell clusters

To test the designed glycopeptide assemblies for inducing morphogenesis in vitro, we use a fibroblast cell line (HS-5<sup>60</sup>) as a simple assay because fibroblast cells synthesize 3D ECM slowly (i.e., requiring days and high cell density to generate 3D ECM) and hardly form spheroids themselves.<sup>1</sup> Incubation a monolayer of HS-5 cells with **1** induces cell spheroids within 24 hours even at the concentration as low as 50  $\mu\text{M}$ , while cells, maintained in medium only, remain as a monolayer (Figure S3a). The maxim size of HS-5 spheroid is about 700  $\mu\text{m}$ , achieved when the concentration of **1** is at 50  $\mu\text{M}$  within 24 hrs.

Exhibiting enhanced fluorescence in an assembled state,<sup>61</sup> NBD reveals the distribution of the assemblies of **1** during the formation of spheroids. In the cell monolayer (Figure 1c), the assemblies mainly locate on cell surfaces, with several large assemblies fluorescing brightly and scattering between the cells. While most of the fluorescent puncta locate within the monolayer, a few of them reside on top of the monolayer (Figure 1c, z-scan stack). Actin staining shows that actin filaments mainly locate at the edge of the stretched cells, much less near the cell-cell contact edges, agreeing with the focal adhesion of these cells to substratum. Moreover, fewer actin filaments appear at the location with higher yellow fluorescence (assemblies of **1**), where cell shapes start to become rounder than the highly spreading cells (Figure 1c), suggesting that the glycopeptide assemblies reduce cell focal adhesion to the substratum, which would favor cell aggregation.<sup>34, 62</sup>

Fluorescent images of a cell spheroid show that much more assemblies present on/in the spheroid than on the monolayer (Figure 1c&1d). Z-scan (Movie S1) reveals that more assemblies present above the bottom layer of the spheroids. The ratio of yellow fluorescence (assemblies of **1**) and the red fluorescence (actin) become highest at the top of the spheroids. Thus, the higher amount of the assemblies of **1** in the spheroids likely originates from (i) cell clustering tend to initiate at the locations with more assemblies, (ii) cells bring the assemblies on their surfaces into the spheroids when migrating towards the spheroids, (iii) the cell spheroids have high cell density, and (iv) smaller spheroids merge to form a larger

one (Movie S2). The majority of the fluorescent assemblies locate extracellularly, resembling ECM between the cells in the entire cell spheroid (Figure 1c and movie S1& S3), confirming that the glycopeptide assemblies functionally enhance intercellular interactions to induce the spheroids. Actin staining (Figure 1d) shows that the cells in spheroids are smaller and rounder, largely favoring the compact cell packing in the spheroids. Cells on the edge of the bottom of the spheroids stretch fully, helping the spheroids attach to the substratum. Fewer actin filaments present on the outmost cells in the middle of the spheroids, agreeing with the lack focal adhesion. Considerable amounts of yellow and red fluorescence co-localize inside the spheroids, indicating the assemblies likely increase intercellular adhesion (fibrillar adhesion<sup>63</sup>). Notably, small nucleus dye Hoechst 33342 barely stains the nuclei inside the cell spheroids after 5-minute incubation, confirming the 3D cell organization.

### Assemblies of the glycopeptides supplement fibronectin

These assemblies of the glycopeptides, with RGD and glycosylation, resemble fibronectin—a glycoprotein that contains RGD<sup>64</sup>— which, together with the integrin,<sup>65, 66</sup> constitutes major recognition molecules for cell adhesion. Thus, the glycopeptide assemblies likely supplement the functions of fibronectin in ECM to interact with cell adhesion proteins on cell membrane and enable 3D cell organization. Immunofluorescence staining of fibronectins in the HS-5 spheroids shows that the assemblies of **1** intertwine with fibronectin, functioning as “fibronectin-like entities” in ECM to enhance cellular adhesion (Figure 2a, Movie S4&S5). That is, fibronectin and **1** co-assemble, and the assemblies of glycopeptides resemble fibronectin in the aspects that they form matrix with RGD as the site of cell attachment.

The above results support the mechanism how HS-5 cells transform from a monolayer to spheroids (Scheme 1, Figure 2b): (i) Petri dish, being able to absorb proteins from serum and cell-derived ECM proteins at later times of culture, acts as the substratum for cell adhesion so that HS-5 cells attach to the surface of the petri dish via cell adhesion proteins binding to the ECM coated on the substratum (e.g., the binding of integrins and fibronectins); (ii) the assemblies, which attach on the cell surfaces, likely by interacting with adhesion molecule (e.g., integrin, E-selectin, cadherins (Figure 2b)). Such assemblies, being nanoparticles at between the cells and the substratum, reduce focal adhesion to help cell detach from the substratum and migrate onto other cells. The cell-cell interaction allows the nanoparticles merge and grow, thus mimicking ECM to enhance intercellular interactions; (iii) More HS-5 cells bring the assemblies on their surfaces to the clusters, leading to a higher local concentration to generate larger assemblies, which attracts more cells nearby to join the 3D clusters or favors small cell clusters to form cell spheroids (Movie S2). This observation also confirms the adaptive feature of the supramolecular assemblies of the glycopeptides.

### The assemblies interact with cell adhesion proteins

To prove the mechanism illustrated in Scheme 1 and Figure 2b, we synthesize Ac-FRGD-glucosamine (**2**), by replacing the NBD-motif in **1** with an acetyl group (Figure 3a). NBD, though as described before is able to promote self-assembly of the peptide[ref], its role in this work is to cap the free N-termini. Because using acetyl (Ac-) achieves the same effect,

NBD is unlikely to be uniquely required for formation of cell spheroids. Molecule **2** self-assembles to form nanostructures (e.g., nanoparticles) and enables the formation of spheroids at the concentration as low as 50  $\mu\text{M}$  (Figures S4&S5). Antibodies against E-/N-cadherin, integrin  $\beta_1/\beta_3/\alpha_v\beta_3$ , and E-selectin all antagonize the activities of the assemblies of **2**, but to different extent, while these mAbs themselves show little effect on the cells (Figures 3b and S5). Anti-E-selectin and anti-N/E-cadherin mAbs exhibit strongest inhibition as they almost prevent the formation of spheroids even at 200  $\mu\text{M}$  of **2**, indicating that the assemblies, indeed, affect the functions of E-selectin and N-/E-cadherins for enhancing cell aggregation. Moreover, the glycopeptide (**2**) at high concentration (>200  $\mu\text{M}$ ) is able to counter the blocking by the antibodies of E-selectin and N-cadherin (Figure 3B), suggesting the interactions between the nanofibers and E-selectin or N-cadherin. Unlike the case of selectin and cadherins, the addition of anti-integrin  $\beta_1$ , with **2** at 500  $\mu\text{M}$ , increases the number of cell clusters, but decreases the number of cell clusters when **2** is 200  $\mu\text{M}$  (and below), agreeing with that the assemblies of **2**, via interacting with the integrins, not only detach the cells from the substratum, but also enhance intercellular interactions. The addition of anti-integrin  $\beta_3/\alpha_v\beta_3$  also slightly inhibits the formation of the spheroids, indicating that endogenous cell-ECM interactions contribute to the spheroids induced by the glycopeptide assemblies. The addition of the inhibitors of these adhesion proteins exhibits similar effect as that of adding the mAbs. EDTA (inhibitor of cadherins) or A205804 (inhibitor of selectin) significantly reduce the number of spheroids, even at 500  $\mu\text{M}$  of **2**. But cilengitide (inhibitor of integrin) remarkably augments the effect of **2** (Figures 3c and S5). Like the reported cyclic RGD derivative, cilengitide itself is able to induce small cell clusters via reducing cell adhesion to substratum, but the prolonged incubation is unable to increase the sizes of the spheroids. This observation agrees with that cilengitide is too small to binds two integrins from different cells simultaneously (i.e., acting as an intercellular bridge). Because their sizes fall into the range of the sizes of macromolecules (e.g., glycoproteins, proteoglycan, and polysaccharide), the continuum of the assemblies of the glycopeptides (e.g., the nanofibers and nanoparticles) should be able to bridge the intercellular space ( $\sim 25$  nm)<sup>67</sup> and enhance intercellular adhesion. Although glucosamine or chondrosine itself is a poor ligand for E-selectin and E/N-cadherins, their assemblies, resulted from the self-assembly of the glycopeptides, are able to behave differently from the monomeric glucosamine and chondrosine. That is, monomeric glucosamine or chondrosine is not a ligand for E-selectin and E/N-cadherins and hardly affects them, while these sugar in assembled state have an effect on the function of these proteins. However, the binding constants between these sugar assemblies and E-selectin and E/N-cadherins remain to be determined. In addition, it is too simple to assume that those glycans only promote self-assembly because the assumption is inconsistent with our previous observation that the addition of glucosamine to peptides disrupt self-assemblies. In addition, MTT assay confirms the cell-compatibility of mAbs and inhibitors at the working concentrations (Figure S6). These results, collectively, support that the assemblies of the glycopeptides, being multifunctional, dynamically interact with cell adhesion proteins (integrins, selectin and cadherins) to promote intercellular interactions for morphogenesis in vitro.

To further confirm the roles of the assemblies, we also examine the distributions of ECM proteins (fibronectin) and endogenous cell adhesion molecule (cadherins, selectin, and

integrin) in the monolayer and the spheroids of HS-5 cells. We use non-fluorescent **2** instead of **1** to avoid fluorescence interference, and image the smaller cell clusters (at initial state) for superior staining since mAbs hardly reach the center of the spheroids. According to Figure 3D, the assemblies of **2** induce the change of the density of these key cell adhesion proteins, but hardly change the density of fibronectin (Figure S7), from the monolayer to spheroids, supporting that the assemblies of the glycopeptides interact with cell adhesion proteins in a way resembling the action of fibronectin. Specifically, few N-cadherins exist on cells in the absence of **2**, while much more N-cadherins accumulate on the cell membrane with the treatment of **2**, indicating that the assemblies of **2** cluster the N-cadherins. In case of other proteins (E-cadherin, E-selectin, integrin  $\beta_1/\beta_3/\alpha_v\beta_3$ ), there are also more green fluorescence in the spheroids than in the monolayers, indicating enhanced cell-ECM interactions in the spheroids induced by the glycopeptide assemblies. In both the monolayers and the spheroids, spatial distributions of actin and integrins largely co-localize, agreeing with that integrin link the ECM to the actin cytoskeleton and transmit biochemical signals and mechanical force across the plasma membrane.<sup>68</sup> Actins and N-cadherins, while hardly co-localizing without the treatment of **2**, co-localize after the formation of the spheroids, indicating that the assemblies of **2**, indeed, promote the intercellular interactions and communications. E-selectin, however, hardly co-localizes with actins both before and after the treatment of **2**.

### Molecular validation of the assemblies

Following the updated view on target validation through molecular design,<sup>69, 70</sup> we design and synthesize the analogs of **1** and **2** for elucidating the role of each segment in the glycopeptides and validating the concept of assemblies of glycopeptides modulating cell adhesion. Scheme 2 shows the general structures of the analogs: **1-9**, consisting of an N-terminal capping, an RGD-containing peptide, and a saccharide, but varying the saccharide (**5** (galactosamine) and **6** (chondrosine)), varying N-capping (NBD-, acetyl (Ac-), adenine (Ade-), and thymine (Thy-)), or elongating the peptide sequence but keeping the RGD domain (**3**, **7** and **8**); **10-12**, lacking saccharide; **13**, lacking RGD domain; **14**, lacking N-terminal capping; and **15**, having an RGE as the control of RGD. After confirming the cell compatibility of all these 15 compounds by cell viability assay (Figure S8), we incubate HS-5 cells with these molecules at 50  $\mu\text{M}$  in culture medium and find that only the N-terminal capped RGD-containing glycopeptides (**1-9**) effectively stimulate the HS-5 cell to form spheroids (Figure 4a). As summarized in Figure 4b, (i) **10-12**, without the saccharide, hardly result in spheroids; (ii) the use of different saccharides (**4**, **5**, and **6**) makes little difference, agreeing with that the assemblies of saccharides can mimic a disparate glycan;<sup>71</sup> (iii) **13**, without the RGD domain, or **15**, with the mutation of RGD to RGE, hardly induces spheroids; (iv) inserting other amino acids but keeping the RGD domain (**3**, **7**, and **8**) barely influence the formation of spheroids, confirming that cell adhesion sequences are another critical segment for the cell aggregation; (v) **14**, containing both the saccharide and RGD domain but no N-terminal capping is ineffective, probably because N-terminal capping is essential for enhancing the self-assembling ability and modifying electronic properties of the glycopeptides. Surprisingly, the mixture of **11** and **13** can stimulate the cell clustering, though **11** or **13** itself is ineffective. However, the mixture of **12** and **13** is ineffective, indicating that certain heterotypic assemblies consisting of RGD domain and saccharides are

able to mimic the function of glycoproteins. Moreover, even at 500  $\mu\text{M}$ , **10-15**, lacking any one of the three motifs, hardly result in cell clustering (Figure 4c). These results validate the indispensable roles of N-terminal capping, cell adhesion sequence, and saccharide for enabling morphogenesis of HS-5 cells *in vitro*.

Live/dead cell assay confirms cells alive in the spheroids since cells in the spheroids grow well after being sub-cultured (Figure 4d). When a micropipette tip, filled with culture medium containing **2** at 500  $\mu\text{M}$ , touches a monolayer of HS-5, spheroids only form at the location of the pipette tip (Figure 4e&4f), indicating that cell clustering initiates at the locations of high local concentrations of the glycopeptides, where supramolecular assemblies form. Cell migration assay shows that the glycopeptide assemblies significantly promote cell migration (Figure 4g&4h), further supporting that the assemblies reduce cell attachment to the substratum.

### Assemblies of the glycopeptides lead to forming cell spheroids

To elucidate the relationship of the concentrations, the extent of self-assembly, and the formation of cell spheroids, we use the static light scattering (SLS) to determine the assemblies of **2**, and find that the intensity of SLS increases nonlinearly with the concentration of **2** (Figure 5a, 5b). The SLS signals of **2** increases dramatically with the decrease of the detection angles (Figure 5a), suggesting non-spherical shapes of the assemblies. The numbers of the cell spheroids are proportional to the intensity of SLS at the detecting angle of 30 degree (Figure 5c), indicating the correlation between the assemblies and the spheroids. Moreover, **2** (500  $\mu\text{M}$ ) combined with Tween-20 (0.025% (a cell compatible concentration), a surfactant that disrupts the assemblies of **2** (Figure 5d), hardly results in any cell spheroids (Figures 5e and S9), validating that it is the assemblies rather than the monomers to induce the cell spheroids. Other glycopeptides that enable the spheroids (**1**, **3-9**) all self-assemble to form nanoscale structures (Figure S10) and to exhibit relatively high SLS intensities (Figure 5f), further validating that the assemblies of the glycopeptides result in the spheroids of HS-5 cells.

### The cell spheroids exhibit drug resistance

The additional dimensionality of cell spheroids resulted from incubation with the glycopeptide assemblies not only influences the spatial organization (i.e., monolayer to spheroids) and morphology of the cells (i.e., long and spreading to round), distribution of surface receptors/proteins (i.e., cadherins, selectin, and integrins), but also imparts physical constraints to the cells, all of which affect the signal transduction, as well as molecular diffusion from the outside to the inside of cell clusters. In fact, we observe the following results: (i) short-time (5 minutes) incubation with nuclei staining dye (Hoechst 33342) is unable to stain efficiently the nuclei of cells inside the spheroids; (ii) mAbs for immunofluorescence staining hardly reach the center of the spheroids; (iii) small molecule dye calcein (for live cell staining) fails to stain the inner cells in the spheroids. All of these results further validate that the cell spheroids, induced by the glycopeptide assemblies, resemble *in vivo* situation and justify the evaluation of the spheroids to cytotoxic drugs.



Obviously, cell density is another factor that affects the formation of spheroids. By varying the initial cell density in a 96-well plate from  $3.0 \times 10^4$  to  $1.0 \times 10^4$  cells/well with a step of 1000 cells, we determine a threshold of  $2.5 \times 10^4$  cells/well that enables cell spheroids after the treatment of **2** (Figure S11). Based on this observation, we design experiments to examine cellular responses to drugs in the spheroids. HS-5 cells in a 96-well plate at initial cell density of  $3.0 \times 10^4$  cells/well and treated with **2** (500  $\mu\text{M}$ ) in culture medium form the spheroids after 24 hours, while the ones at the same density maintained in medium only remain as a monolayer. After the formation of the spheroids, the survival of HS-5 increases by 30% in the presence of cisplatin (100  $\mu\text{M}$ ), and the  $\text{IC}_{50}$  increases about 10  $\mu\text{M}$  (Figure 6a). Similarly, the cell survival increases by more than 30% upon the addition of doxorubicin, and the  $\text{IC}_{50}$  increases by 140 nM (Figure 6c). Although the change in  $\text{IC}_{50}$  is relatively small, but the protection resulted from the formation of spheroids is obvious and statistically significant when the drugs present at high concentrations. These observation supports the enhanced protection of cells by the spheroids. In another control experiment (initial cell number to  $1.0 \times 10^4$  cells/well and the addition of **2** (500  $\mu\text{M}$ ) hardly leads to cell clustering, Figure 6b&bd), there is little difference regarding the cytotoxicity of cisplatin and doxorubicin against HS-5 cells, comparing to without the addition of **2**. As summarized in Figure 6e, these results confirm that the formation of spheroids efficiently decreases the drug sensitivity of the cells.

## Conclusion

In this work, we validate the assemblies of readily accessible glycopeptides (e.g., **1-9**) for promoting morphogenesis in vitro. One unique feature of the assemblies is that there are adaptive (i.e., context-dependent) according to the environment of their formation. For molecules **1-9**, higher concentration usually leads to more spheroids, suggesting increasing the self-assembling ability of the glycopeptides likely results in more effective assemblies for promoting morphogenesis in vitro. Though the binding constants of the E-selectin and N/E-cadherins with the sugars in the assemblies remain to be determined, antagonistic mAb or inhibitors to N/E-cadherins, E-selectin, integrins significantly counter the effects of the assemblies, indicating the effects of these glycopeptide assemblies on the adhesion proteins, which further implies these glycopeptide assemblies behave more like multifunctional entities in extracellular space for the cell spheroids. Since the equilibrium of self-assembly allows the existence of smaller aggregates (or particles or oligomers) of the glycopeptides, these small aggregates compete with the substratum to interact with integrins, thus reduce focal adhesion to the substratum, which actually accelerates or facilitates the cell aggregation. Thus, even being generated from a single molecular species, the assemblies are able to modulate cell adhesions, which involve many signals. This ability implies the assemblies generate different signals, likely originated from the assemblies with a size continuum from nanoparticles to nanofibers in the dimensions of biomacromolecules. This mechanism is supported by the function of cilengitide, which effectively binds integrins to reduce focal adhesion, but is unable to block the spheroids induced by the glycopeptide assemblies.

Unlike 3D scaffolds (polymeric hydrogels) for 3D cell in vitro model or generating cell spheroids by cyclic RGD derivative and agarose surface, this work, for the first time, reports

the use of conformable nanoscale assemblies of a single molecular species to initiate in vitro morphogenesis without requiring an *a priori* 3D architecture, mechanical modulations, or agarose surface. This situation is more consistent with cell morphogenesis occurred in nature, especially in the case of embryogenesis. The use of glycopeptide assemblies not only reduces the synthetic burden of building a glycosylated 3D scaffold, but also generates cell spheroids that more closely resemble in vivo tumors, which are heavily glycosylated, compact in cell packing, heterogeneous, and drug resistant. Moreover, this approach is also applicable to generate spheroids of cells other than HS-5, such as OVSCAR-3 cells (Figure S12). In addition, the assemblies of glycopeptides carry more functions than fibronectin, since using same amount of fibronectin (0.05 wt%) hardly lead to the formation of cell spheroids. Of course, this approach remains to be improved in the future. One future application is to use this approach to generate dynamic molecular assemblies<sup>72</sup> for forming heterogeneous spheroids that mimic organs or regenerate organs.

## Supplementary Material

Refer to Web version on PubMed Central for supplementary material.

## Acknowledgments

This work is partially supported by NIH (R01CA142746), the W.M. Keck Foundation, NSF (DMR-1420382). J.Z. is an HHMI International Research Fellow. We thank Shiyu Wang, Mugdha Deshpande, and Avital Rodal's help for setting up life imaging incubator on confocal microscope. We thank Beverly Torok-Storb for providing HS-5 cells.

## References

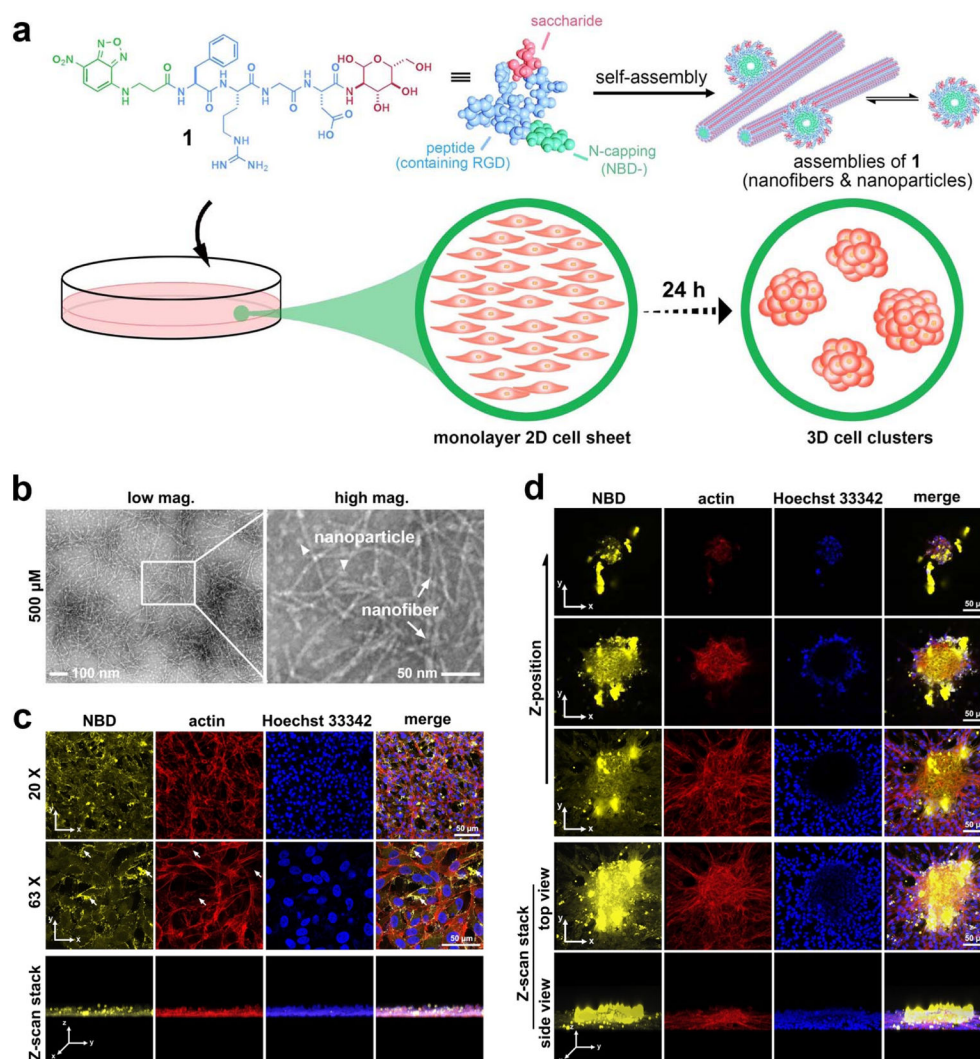
1. Cukierman E, Pankov R, Stevens DR, Yamada KM. Taking cell-matrix adhesions to the third dimension. *Science*. 2001; 294:1708–1712. [PubMed: 11721053]
2. Imamura Y, Mukohara T, Shimono Y, Funakoshi Y, Chayahara N, Toyoda M, Kiyota N, Takao S, Kono S, Nakatsura T, Minami H. Comparison of 2D- and 3D-culture models as drug-testing platforms in breast cancer. *Oncol Rep*. 2015; 33:1837–1843. [PubMed: 25634491]
3. Falconnet D, Csucs G, Grandin HM, Textor M. Surface engineering approaches to micropattern surfaces for cell-based assays. *Biomaterials*. 2006; 27:3044–3063. [PubMed: 16458351]
4. Birgersdotter A, Sandberg R, Ernberg I. Gene expression perturbation in vitro--a growing case for three-dimensional (3D) culture systems. *Semin Cancer Biol*. 2005; 15:405–412. [PubMed: 16055341]
5. Weaver VM, Petersen OW, Wang F, Larabell CA, Briand P, Damsky C, Bissell MJ. Reversion of the malignant phenotype of human breast cells in three-dimensional culture and in vivo by integrin blocking antibodies. *J Cell Biol*. 1997; 137:231–245. [PubMed: 9105051]
6. Bhadriraju K, Chen CS. Engineering cellular microenvironments to improve cell-based drug testing. *Drug Discov Today*. 2002; 7:612–620. [PubMed: 12047872]
7. Yamada KM, Cukierman E. Modeling tissue morphogenesis and cancer in 3D. *Cell*. 2007; 130:601–610. [PubMed: 17719539]
8. Baharvand H, Hashemi SM, Ashtiani SK, Farrokhi A. Differentiation of human embryonic stem cells into hepatocytes in 2D and 3D culture systems in vitro. *Int J Dev Biol*. 2006; 50:645–652. [PubMed: 16892178]
9. Benya PD, Shaffer JD. Dedifferentiated chondrocytes reexpress the differentiated collagen phenotype when cultured in agarose gels. *Cell*. 1982; 30:215–224. [PubMed: 7127471]
10. Nelson CM, Bissell MJ. Modeling dynamic reciprocity: engineering three-dimensional culture models of breast architecture, function, and neoplastic transformation. *Semin Cancer Biol*. 2005; 15:342–352. [PubMed: 15963732]

11. Tsoi AM, Zaitseva-Zotova DS, Edel'veis EF, Bartkoviak A, Gorzhen ZL, Vodovozova EL, Markvicheva EA. Microencapsulated multicellular tumor spheroids: preparation and use as a novel in vitro model for drug screening. *Biomed Khim.* 2010; 56:674–685. [PubMed: 21395070]
12. Nishiguchi A, Yoshida H, Matsusaki M, Akashi M. Rapid Construction of Three-Dimensional Multilayered Tissues with Endothelial Tube Networks by the Cell-Accumulation Technique. *Adv Mater.* 2011; 23:3506–3510. [PubMed: 21728193]
13. Liu Y, Sakai S, Taya M. Engineering tissues with a perfusable vessel-like network using endothelialized alginate hydrogel fiber and spheroid-enclosing microcapsules. *Heliyon.* 2016; 2:e00067. [PubMed: 27441246]
14. Youn W, Ko EH, Kim MH, Park M, Hong D, Seisenbaeva GA, Kessler VG, Choi IS. Cytoprotective Encapsulation of Individual Jurkat T Cells within Durable TiO<sub>2</sub> Shells for T-Cell Therapy. *Angew Chem Int Ed.* 2017; 56:10609.
15. Derda R, Laromaine A, Mammoto A, Tang SKY, Mammoto T, Ingber DE, Whitesides GM. Paper-supported 3D cell culture for tissue-based bioassays. *Proc Natl Acad Sci U S A.* 2009; 106:18457–18462. S18457/18451–S18457/18459. [PubMed: 19846768]
16. Loessner D, Meinert C, Kaemmerer E, Martine LC, Yue K, Levett PA, Klein TJ, Melchels FPW, Khademhosseini A, Hutmacher DW. Functionalization, preparation and use of cell-laden gelatin methacryloyl-based hydrogels as modular tissue culture platforms. *Nat Protoc.* 2016; 11:727–746. [PubMed: 26985572]
17. Jayawarna V, Ali M, Jowitt TA, Miller AF, Saiani A, Gough JE, Ulijn RV. Nanostructured hydrogels for three-dimensional cell culture through self-assembly of fluorenylmethoxycarbonyldipeptides. *Adv Mater (Weinheim, Ger).* 2006; 18:611–614.
18. Alakpa EV, Jayawarna V, Lampel A, Burgess KV, West CC, Bakker SCJ, Roy S, Javid N, Fleming S, Lamprou DA, Yang J, Miller A, Urquhart AJ, Frederix PWJM, Hunt NT, Peault B, Ulijn RV, Dalby MJ. Tunable Supramolecular Hydrogels for Selection of Lineage-Guiding Metabolites in Stem Cell Cultures. *Chem.* 2016; 1:512.
19. Silva GA, Czeisler C, Niece KL, Beniash E, Harrington DA, Kessler JA, Stupp SI. Selective differentiation of neural progenitor cells by high-epitope density nanofibers. *Science (Washington, DC, U S ).* 2004; 303:1352–1355.
20. Knight E, Przyborski S. Advances in 3D cell culture technologies enabling tissue-like structures to be created in vitro. *J Anat.* 2015; 227:746–756. [PubMed: 25411113]
21. Edmondson R, Broglie JJ, Adcock AF, Yang L. Three-Dimensional Cell Culture Systems and Their Applications in Drug Discovery and Cell-Based Biosensors. *Assay Drug Dev Technol.* 2014; 12:207–218. [PubMed: 24831787]
22. Desai N, Rambhia P, Gishto A. Human embryonic stem cell cultivation: historical perspective and evolution of xeno-free culture systems. *Reprod Biol Endocrinol.* 2015; 13:9/1–9/30. [PubMed: 25890180]
23. Shuhendler AJ, Prasad P, Cai P, Hui KKW, Henderson JT, Rauth AM, Wu XY. Matrigel alters the pathophysiology of orthotopic human breast adenocarcinoma xenografts with implications for nanomedicine evaluation. *Nanomedicine (N Y, NY, U S ).* 2013; 9:795–805.
24. Vaillant F, Lindeman GJ, Visvader JE. Jekyll or Hyde: does Matrigel provide a more or less physiological environment in mammary repopulating assays? *Breast Cancer Res.* 2011; 13:108. [PubMed: 21635708]
25. Rookmaaker MB, Schutgens F, Verhaar MC, Clevers H. Development and application of human adult stem or progenitor cell organoids. *Nat Rev Nephrol.* 2015; 11:546–554. [PubMed: 26215513]
26. Gao D, Vela I, Sboner A, Iaquina PJ, Karthaus WR, Gopalan A, Dowling C, Wanjala JN, Undvall EA, Arora VK, Wongvipat J, Kossai M, Ramazanoglu S, Barboza LP, Di W, Cao Z, Zhang QF, Sirota I, Ran L, MacDonald TY, Beltran H, Mosquera J-M, Touijer KA, Scardino PT, Laudone VP, Curtis KR, Rathkopf DE, Morris MJ, Danila DC, Slovin SF, Solomon SB, Eastham JA, Chi P, Carver B, Rubin MA, Scher HI, Clevers H, Sawyers CL, Chen Y. Organoid Cultures Derived from Patients with Advanced Prostate Cancer. *Cell.* 2014; 159:176–187. [PubMed: 25201530]
27. Karthaus WR, Iaquina PJ, Drost J, Gracanin A, Van Boxtel R, Wongvipat J, Dowling CM, Gao D, Begthel H, Sachs N, Vries RGJ, Cuppen E, Chen Y, Sawyers CL, Clevers HC. Identification of

- Multipotent Luminal Progenitor Cells in Human Prostate Organoid Cultures. *Cell*. 2014; 159:163–175. [PubMed: 25201529]
28. Drost J, Karthaus WR, Gao D, Driehuis E, Sawyers CL, Chen Y, Clevers H. Organoid culture systems for prostate epithelial and cancer tissue. *Nat Protoc*. 2016; 11:347–358. [PubMed: 26797458]
  29. Kelm JM, Timmins NE, Brown CJ, Fussenegger M, Nielsen LK. Method for generation of homogeneous multicellular tumor spheroids applicable to a wide variety of cell types. *Biotechnology and Bioengineering*. 2003; 83:173–180. [PubMed: 12768623]
  30. Frith JE, Thomson B, Genever PG. Dynamic Three-Dimensional Culture Methods Enhance Mesenchymal Stem Cell Properties and Increase Therapeutic Potential. *Tissue Eng Part C Methods*. 2010; 16:735–749. [PubMed: 19811095]
  31. Zheng HX, Tian WM, Yan HJ, Yue L, Zhang Y, Han FT, Chen XB, Li Y. Rotary culture promotes the proliferation of MCF-7 cells encapsulated in three-dimensional collagen-alginate hydrogels via activation of the ERK1/2-MAPK pathway. *Biomedical Materials*. 2012; 7:10.
  32. Raghavan S, Mehta P, Horst EN, Ward MR, Rowley KR, Mehta G. Comparative analysis of tumor spheroid generation techniques for differential in vitro drug toxicity. *Oncotarget*. 2016; 7:16948–16961. [PubMed: 26918944]
  33. Gumbiner BM. Cell adhesion: The molecular basis of tissue architecture and morphogenesis. *Cell*. 1996; 84:345–357. [PubMed: 8608588]
  34. Powers MJ, Griffith LG. Adhesion-guided in vitro morphogenesis in pure and mixed cell cultures. *Microsc Res Tech*. 1998; 43:379–384. [PubMed: 9858335]
  35. Powers MJ, Rodriguez RE, Griffith LG. Cell-substratum adhesion strength as a determinant of hepatocyte aggregate morphology. *Biotechnology and Bioengineering*. 1997; 53:415–426. [PubMed: 18634032]
  36. Zhang S, Holmes TC, DiPersio CM, Hynes RO, Su X, Rich A. Self-complementary oligopeptide matrices support mammalian cell attachment. *Biomaterials*. 1995; 16:1385–1393. [PubMed: 8590765]
  37. Sargeant TD, Rao MS, Koh C-Y, Stupp SI. Covalent functionalization of NiTi surfaces with bioactive peptide amphiphile nanofibers. *Biomaterials*. 2008; 29:1085–1098. [PubMed: 18083225]
  38. Yamada KM. Adhesive recognition sequences. *J Biol Chem*. 1991; 266:12809–12812. [PubMed: 2071570]
  39. Hynes RO. Integrins: versatility, modulation, and signaling in cell adhesion. *Cell*. 1992; 69:11–25. [PubMed: 1555235]
  40. Akasov R, Zaytseva-Zotova D, Burov S, Leko M, Dontenwill M, Chipier M, Vandamme T, Markvicheva E. Formation of multicellular tumor spheroids induced by cyclic RGD-peptides and use for anticancer drug testing in vitro. *Int J Pharm*. 2016; 506:148–157. [PubMed: 27107900]
  41. Frisco-Cabanos HL, Watanabe M, Okumura N, Kusamori K, Takemoto N, Takaya J, Sato S, Yamazoe S, Takakura Y, Kinoshita S, Nishikawa M, Koizumi N, Uesugi M. Synthetic molecules that protect cells from anoikis and their use in cell transplantation. *Angew Chem Int Ed*. 2014; 53:11208–11213.
  42. Akasov R, Haq S, Haxho F, Samuel V, Burov SV, Markvicheva E, Neufeld RJ, Szewczuk MR. Sialylation transmogrifies human breast and pancreatic cancer cells into 3D multicellular tumor spheroids using cyclic RGD-peptide induced self-assembly. *Oncotarget*. 2016; 7:66119–66134. [PubMed: 27608845]
  43. Haq S, Samuel V, Haxho F, Akasov R, Leko M, Burov SV, Markvicheva E, Szewczuk MR. Sialylation facilitates self-assembly of 3D multicellular prostaspheres by using cyclo-RGDFK(TPP) peptide. *Onco Targets Ther*. 2017; 10:2427–2447. [PubMed: 28496342]
  44. Wang H, Shi J, Feng Z, Zhou R, Xu B, Wang S, Rodal AA. An in situ Dynamic Continuum of Supramolecular Phosphoglycopeptides Enables Formation of 3D Cell Spheroids. *Angew Chem Int Ed*. 2017; 56:7579–7583.
  45. Discher DE, Janmey P, Wang YL. Tissue cells feel and respond to the stiffness of their substrate. *Science*. 2005; 310:1139–1143. [PubMed: 16293750]
  46. Sternlicht MD, Werb Z. How matrix metalloproteinases regulate cell behavior. *Annu Rev Cell Dev Biol*. 2001; 17:463–516. [PubMed: 11687497]

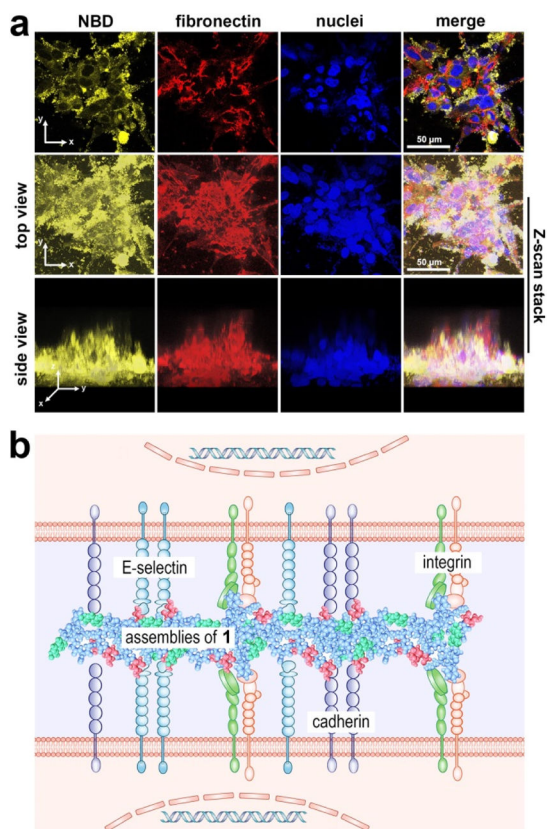
47. Condeelis J, Pollard JW. Macrophages: Obligate partners for tumor cell migration, invasion, and metastasis. *Cell*. 2006; 124:263–266. [PubMed: 16439202]
48. Mouw JK, Ou G, Weaver VM. Extracellular matrix assembly: a multiscale deconstruction. *Nat Rev Mol Cell Biol*. 2014; 15:771–785. [PubMed: 25370693]
49. Bonnans C, Chou J, Werb Z. Remodelling the extracellular matrix in development and disease. *Nat Rev Mol Cell Biol*. 2014; 15:786–801. [PubMed: 25415508]
50. Reticker-Flynn NE, Braga Malta DF, Winslow MM, Lamar JM, Xu MJ, Underhill GH, Hynes RO, Jacks TE, Bhatia SN. A combinatorial extracellular matrix platform identifies cell-extracellular matrix interactions that correlate with metastasis. *Nat Commun*. 2012; 3:2128/2121–2128/2112.
51. Seo J, Shin J-Y, Leijten J, Jeon O, Camci-Unal G, Dikina AD, Brinegar K, Ghaemmaghami AM, Alsborg E, Khademhosseini A. High-throughput approaches for screening and analysis of cell behaviors. *Biomaterials*. 2018; 153:85–101. [PubMed: 29079207]
52. Sangabathuni S, Murthy RV, Gade M, Bavireddi H, Toraskar S, Sonar MV, Ganesh KN, Kikkeri R. Modeling Glyco-Collagen Conjugates Using a Host-Guest Strategy To Alter Phenotypic Cell Migration and in Vivo Wound Healing. *ACS Nano*. 2017; 11:11969–11977. [PubMed: 29077384]
53. Niu Y, Xie T, Ge K, Lin Y, Lu S. Effects of extracellular matrix glycosylation on proliferation and apoptosis of human dermal fibroblasts via the receptor for advanced glycosylated end products. *Am J Dermatopathol*. 2008; 30:344–351. [PubMed: 18645306]
54. Varki A. Selectin ligands. *Proc Natl Acad Sci U S A*. 1994; 91:7390–7397. [PubMed: 7519775]
55. Ruoslahti E, Pierschbacher MD. New perspectives in cell adhesion: RGD and integrins. *Science*. 1987; 238:491–497. [PubMed: 2821619]
56. Mas-Moruno C, Rechenmacher F, Kessler H. Cilengitide: The First Anti-Angiogenic Small Molecule Drug Candidate. Design, Synthesis and Clinical Evaluation. *Anti-Cancer Agents Med Chem*. 2010; 10:753–768.
57. Reynolds AR, Hart IR, Watson AR, Welti JC, Silva RG, Robinson SD, Da Violante G, Gourlaouen M, Salih M, Jones MC, Jones DT, Saunders G, Kostourou V, Perron-Sierra F, Norman JC, Tucker GC, HodiVala-Dilke KM. Stimulation of tumor growth and angiogenesis by low concentrations of RGD-mimetic integrin inhibitors. *Nat Med*. 2009; 15:392–400. [PubMed: 19305413]
58. Li X, Du X, Gao Y, Shi J, Kuang Y, Xu B. Supramolecular hydrogels formed by the conjugates of nucleobases, Arg-Gly-Asp (RGD) peptides, and glucosamine. *Soft Matter*. 2012; 8:7402–7407. [PubMed: 22844343]
59. Li X, Du X, Li J, Gao Y, Pan Y, Shi J, Zhou N, Xu B. Introducing D-amino acid or simple glycoside into small peptides to enable supramolecular hydrogelators to resist proteolysis. *Langmuir*. 2012; 28:13512–13517. [PubMed: 22906360]
60. Roecklein BA, Torokstorb B. Functionally distinct human marrow stromal cell lines immortalized by transduction with the human papilloma virus E6/E7 genes. *Blood*. 1995; 85:997–1005. [PubMed: 7849321]
61. Gao Y, Shi J, Yuan D, Xu B. Imaging enzyme-triggered self-assembly of small molecules inside live cells. *Nat Commun*. 2012; 3:2040/2041–2040/2048.
62. Powers MJ, Griffith LG. Adhesion-guided in vitro morphogenesis in pure and mixed cell cultures. *Microsc Res Tech*. 1998; 43:379–384. [PubMed: 9858335]
63. Geiger B, Yamada KM. Molecular architecture and function of matrix adhesions. *Cold Spring Harbor Perspect Biol*. 2011; 3:a005033/005031–a005033/005021.
64. Leahy DJ, Aukhil I, Erickson HP. 2.0 angstrom crystal structure of a four-domain segment of human fibronectin encompassing the RGD loop and synergy region. *Cell*. 1996; 84:155–164. [PubMed: 8548820]
65. Guan JL, Trevithick JE, Hynes RO. Fibronectin/integrin interaction induces tyrosine phosphorylation of a 120-kDa protein. *Cell Reg*. 1991; 2:951–964.
66. Mosher DF, Saksela O, Kesioja J, Vaheri A. Distribution of a major surface-associated glycoprotein, fibronectin, in cultures of adherent cells. *J Cell Biochem*. 1977; 6:551–557.
67. Farquhar MG, Palade GE. Junctional complexes in various epithelia. *J Cell Biol*. 1963; 17:375. [PubMed: 13944428]
68. Calderwood DA, Shattil SJ, Ginsberg MH. Integrins and actin filaments: Reciprocal regulation of cell adhesion and signaling. *J Biol Chem*. 2000; 275:22607–22610. [PubMed: 10801899]

69. Sweis RF. Target (In)Validation: A Critical, Sometimes Unheralded, Role of Modern Medicinal Chemistry. *ACS Med Chem Lett.* 2015; 6:618–621. [PubMed: 26101559]
70. Weiss WA, Taylor SS, Shokat KM. Recognizing and exploiting differences between RNAi and small-molecule inhibitors. *Nat Chem Biol.* 2007; 3:739–744. [PubMed: 18007642]
71. Cohen M, Varki A. Modulation of Glycan Recognition by Clustered Saccharide Patches. In: Jeon KW, editor *Modulation of Glycan Recognition by Clustered Saccharide Patches.* Elsevier Academic Press Inc; San Diego: 2014. 75–125.
72. Epstein IR, Xu B. Reaction-diffusion processes at the nano- and microscales. *Nat Nanotechnol.* 2016; 11:312–319. [PubMed: 27045215]



**Figure 1.**

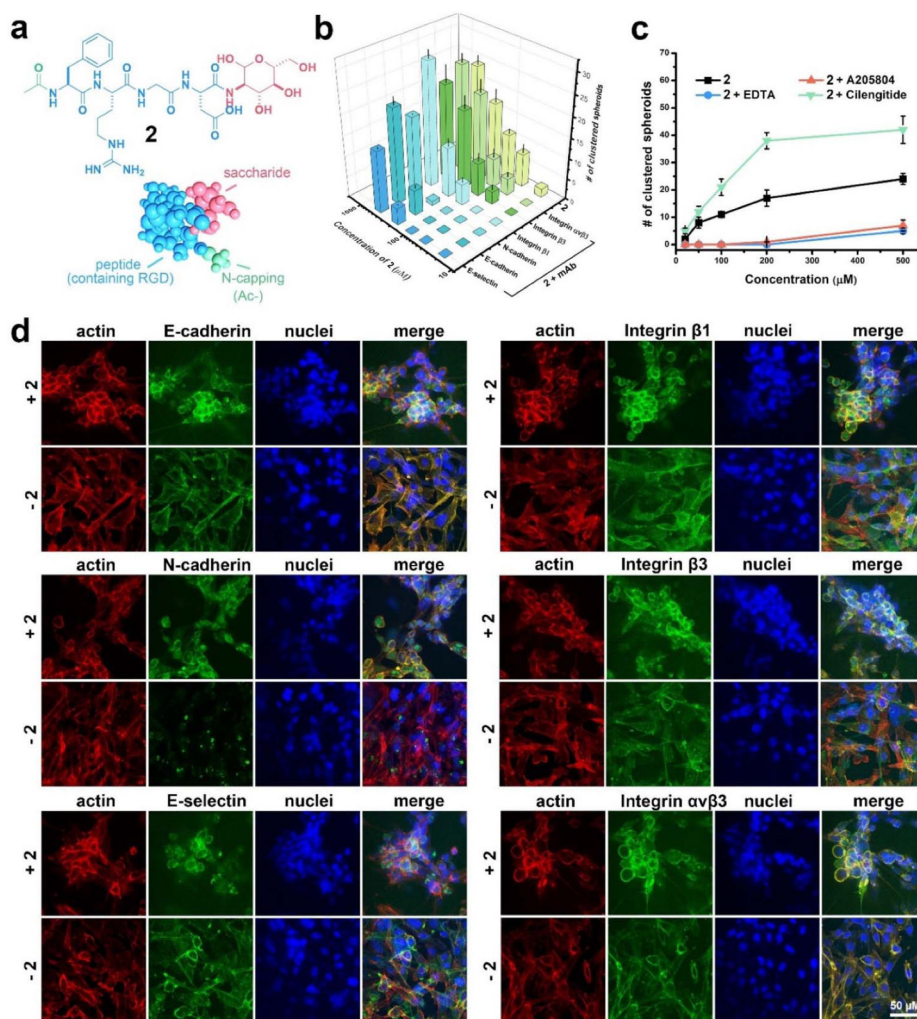
The glycopeptide assemblies attach to the cell surfaces to induce cell spheroids. (a) Schematic illustration of small glycopeptide assemblies (i.e., nanoparticles and nanofibers) to induce the *in vitro* morphogenesis. The glycopeptides (e.g., **1**) consist of N-terminal capping motif (2-(4-nitro-2,1,3-benzoxadiazol-7-yl)-(NBD-)), RGD (integrin-binding domain), and glucosamine (a saccharide). (b) Transmission electron microscope images show nanoparticles (arrow head,  $d = 12 \pm 2$  nm) and nanofibers (arrow,  $d = 5 \pm 2$  nm) in the solution of **1** (500  $\mu$ M, pH 7.4, in water). The scale bar is 100 nm (left) and 50 nm (right). (c) (d) Confocal microscope images of HS-5 cells treated with **1** (500  $\mu$ M) in culture medium for 24 hours. (c) shows the monolayer by imaging the spot/location where there is no cell spheroids while (d) shows the spheroids. Actin is stained for visualizing cell morphologies. Nuclei are stained with Hoechst 33342. The white arrow in (c) shows fewer actin filaments appear at the highly yellow fluorescent spots. The scale bars (in (c) and (d)) are 50  $\mu$ m.



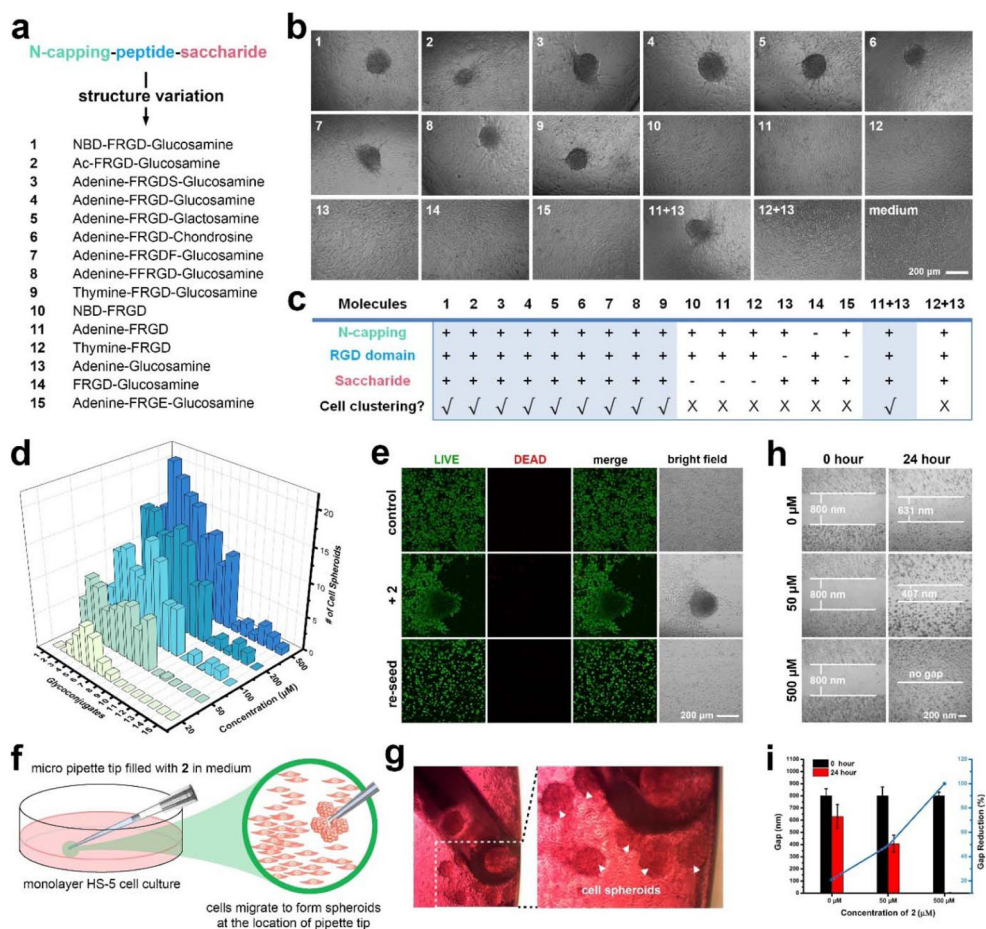
**Figure 2.**

The supramolecular assemblies of the glycopeptides mimic the functions of extracellular matrix components (e.g., fibronectin) to enable cell spheroids. (a) Confocal microscope images of HS-5 cell clusters formed after the treatment of **1** (500 μM) in culture medium for 24 hours. Cell was immunostained with fibronectin mAb prior to imaging. Nuclei were stained with Hoechst 33342. The scale bar is 50 μm. (b) Schematic illustration of the supramolecular assemblies of the glycopeptides interacting with cell adhesion proteins (i.e., integrins, E-selectin, and cadherins).





**Figure 3.** Supramolecular assemblies of the glycopeptides interact with cell adhesion proteins (i.e., integrin, selectin and cadherin) on cell membrane, promoting intercellular interactions and leading to the cell spheroids. (a) Chemical structure of **2**, a non-fluorescent analog of **1**, consisting of N-terminal capping (acetyl), integrin binding domain (RGD), and saccharide (glucosamine). (b) The addition of monoclonal antibodies (mAb) to C- and N-cadherin, E-selectin and integrin  $\beta_1$ ,  $\beta_3$ ,  $\alpha_v\beta_1$  (i.e., anti-C- and N-cadherin, anti-E-selectin and anti-integrin  $\beta_1$ ,  $\beta_3$ ,  $\alpha_v\beta_1$ ) into the HS-5 cell culture inhibits the formation of cell spheroids. (c) The addition of small molecule inhibitors to cadherin and E-selectin (i.e., EDTA and A205804) into the HS-5 cell culture efficiently inhibits the formation of spheroids, while the addition of inhibitor to integrin (i.e., cilengitide) shows opposite effect. (d) Immunofluorescence antibody staining reveals the distribution of membrane proteins that are related with cell adhesion (C- and N-cadherins, E-selectin and Integrin  $\beta_1$ ,  $\beta_3$ ,  $\alpha_v\beta_1$ ) on HS-5 cells treated with and without **2** (500  $\mu$ M) in culture medium for 24 hours. The scale bar is 50  $\mu$ m.

**Figure 4.**

Multifunctional small glycopeptides containing N-terminal capping, glycosylation and RGD integrin-binding domain enable cell spheroids. (a) The architecture of multifunctional small glycopeptides and the control analogs (see Scheme 2 for specific chemical structures). Ac: acetyl; F: phenylalanine; R: arginine; D: aspartic acid; S: serine; E: glutamic acid; NBD: 2-(4-nitro-2,1,3-benzoxadiazol-7-yl)-; (b) Optical images of HS-5 cells incubated with different molecules (1-15) at the concentration of 50  $\mu\text{M}$  for 24 hours. The initial cell number is  $3.0 \times 10^4$ /well in a 96-well plate. The scale bar is 100  $\mu\text{m}$ . Molecules **1-9** alone and **11+13** combination are able to induce HS-5 cell clustering. (c) Table summary regarding chemical structures *v.s.* spheroids, indicating the importance of N-terminal capping, glycosylation, and integrin-binding domain for the observed *in vitro* morphogenesis. (d) Quantification of the numbers of HS-5 clusters formed after the treatment of different small molecules (**1-15**) at multiple concentrations (20, 50, 100, 200, 500  $\mu\text{M}$ ) for 24 h. The initial cell number is  $3.0 \times 10^4$ /well in a 96-well plate. (e) LIVE/DEAD cell assay of HS-5 cells treated with medium only, **2** (100  $\mu\text{M}$ ) in medium, and HS-5 cells in spheroids being lysed and reseeded. The incubation time is 24 hour. The initial number of cells is  $5.0 \times 10^5$ /well in a 35-mm confocal dish. The scale bar is 100  $\mu\text{m}$ . (f) (g) Schematic illustration and optical images of HS-5 spheroids selectively form at the location of the micropipette tips (filled with medium containing 500  $\mu\text{M}$  compound **2**). (h) (i) Cell migration assay of monolayer

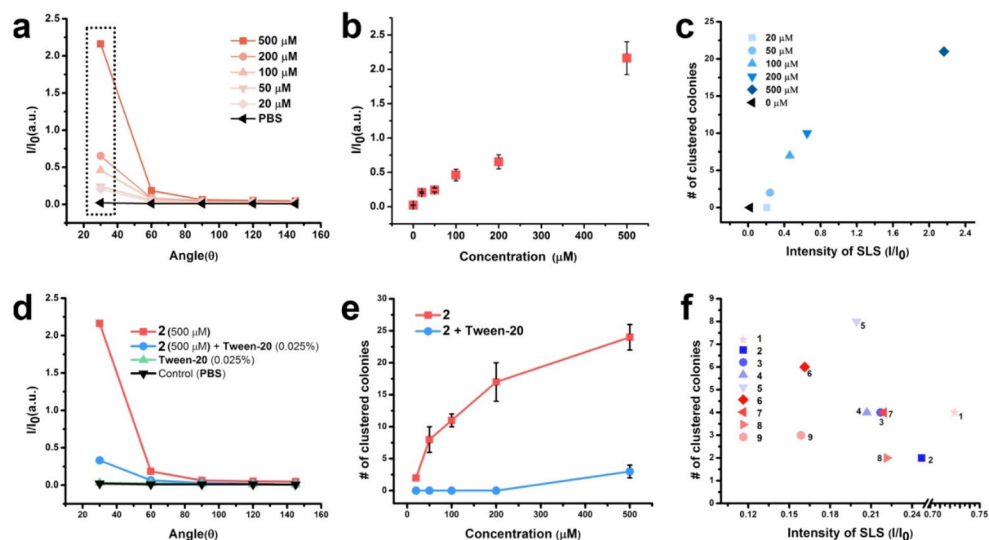
HS-5 cells (80 % confluence) treated with **2** (50 and 500  $\mu\text{M}$ ). The size of the gap was measured both before and after incubation with **2** for 24 hours.

Author Manuscript

Author Manuscript

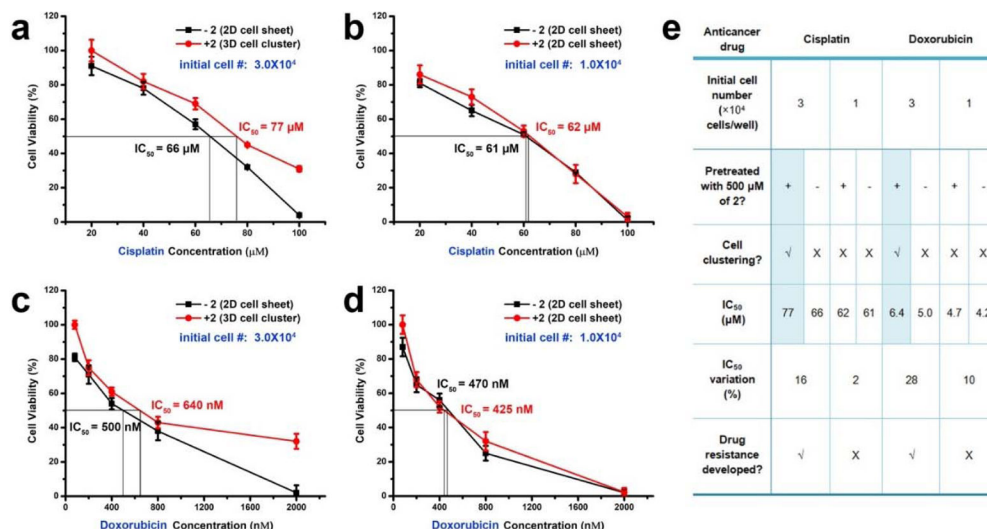
Author Manuscript

Author Manuscript

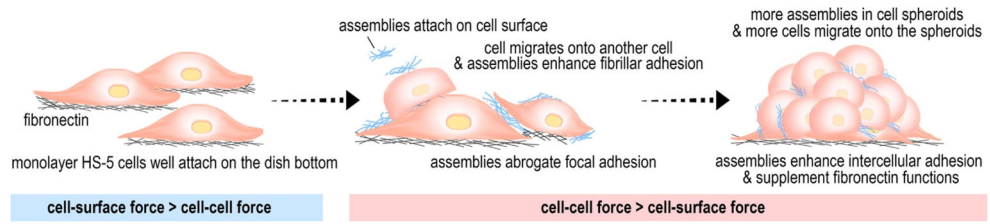


**Figure 5.**

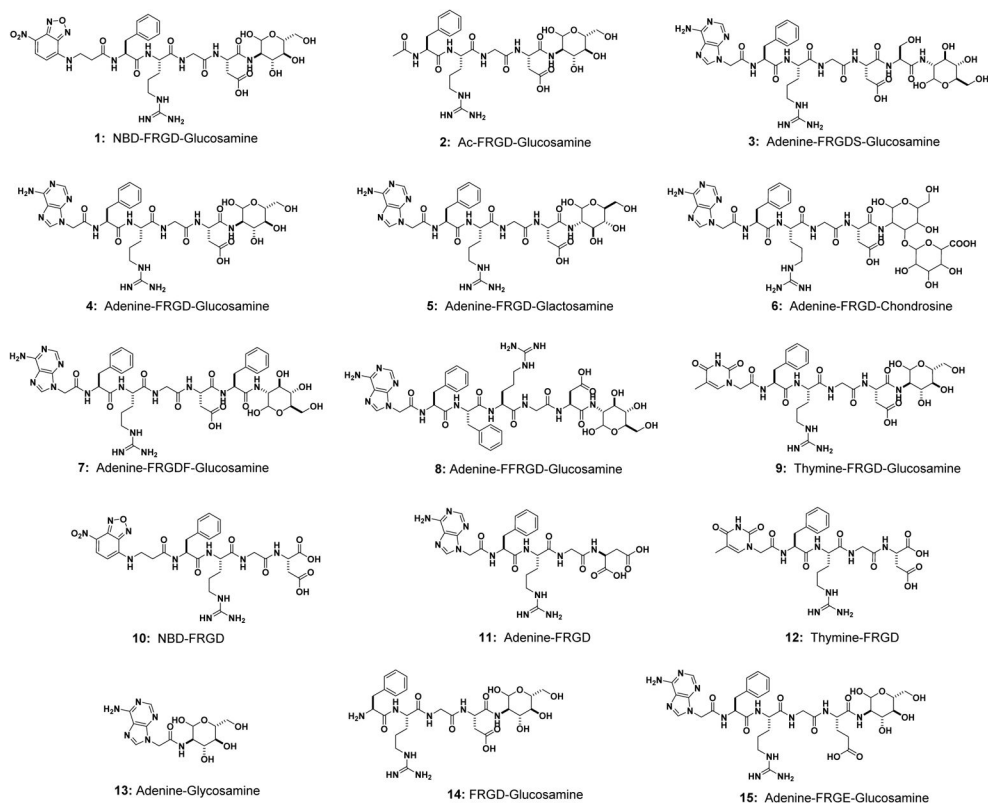
The assemblies, not the monomers, of the multifunctional glycopeptides facilitate the spheroids formation. (a) Static light scattering (SLS) signals of the solutions of **2** at different concentrations (20, 50, 100, 200, 500  $\mu\text{M}$ ), pH = 7.4, detecting angle = 30, 60, 90, 120°. (b) The intensity of the static light scattering (SLS) of **2** vs the different concentrations. Detecting angle = 30° (c) The numbers of HS-5 spheroids are largely positively correlated with 30°-SLS signals of **2** at different concentrations. (d) The SLS intensities of the solutions of **2** (500  $\mu\text{M}$ ), **2** (500  $\mu\text{M}$ ) + Tween-20 (0.025%), Tween-20 (0.025%) alone, and PBS buffer at different detection angles. The addition of detergent breaks down the assemblies of **2** into oligomers or monomers. (e) Removing the assembly by Tween-20 reverts the cells from spheroids to monolayer, indicating the importance of the assemblies for the observation and the transient nature of the action of the assemblies. (f) The plot of the numbers of HS-5 cell spheroids vs 30°-SLS of small molecules **1-9** solutions at the concentration of 50  $\mu\text{M}$ .



**Figure 6.** The cell spheroids exhibit drug resistance. (a) (b) (c) (d) Cell viability of HS-5 treated by (a) (b) cisplatin (c) (c) doxorubicin. The initial cell number is (a) (c)  $3.0 \times 10^4$  and (b) (d)  $1.0 \times 10^4$  cells/well in a 96-well plate. The cells are pretreated with or without **2** (500  $\mu\text{M}$ ) for facilitating the formation of cell spheroids. (e) Summary of the results presented in (a–d).

**Scheme 1.**

Supramolecular assemblies of glycopeptides reduce cell-substratum adhesion and enhance intercellular adhesion, thus result in cell spheroids from a cell monolayer.



**Scheme 2.**

Chemical structures of the multifunctional small glycoconjugates or glycopeptides and some control analogs (1-15).